

# Solution-Processed and High-Performance Organic Solar Cells Using Small Molecules with a Benzodithiophene Unit

Jiaoyan Zhou,<sup>†</sup> Yi Zuo,<sup>†</sup> Xiangjian Wan,<sup>†</sup> Guankui Long, Qian Zhang, Wang Ni, Yongsheng Liu, Zhi Li, Guangrui He, Chenxi Li, Bin Kan, Miaomiao Li, and Yongsheng Chen\*

Key Laboratory for Functional Polymer Materials and Centre for Nanoscale Science and Technology, Institute of Polymer Chemistry, College of Chemistry, Nankai University, Tianjin 300071, China

**S** Supporting Information

**ABSTRACT:** Three small molecules named DR3TBDTT, DR3TBDTT-HD, and DR3TBD2T with a benzo[1,2-*b*:4,5-*b'*]dithiophene (BDT) unit as the central building block have been designed and synthesized for solution-processed bulk-heterojunction solar cells. Power conversion efficiencies (PCEs) of 8.12% (certified 7.61%) and 8.02% under AM 1.5G irradiation (100 mW cm<sup>-2</sup>) have been achieved for DR3TBDTT- and DR3TBD2T-based organic photovoltaic devices (OPVs) with PC<sub>71</sub>BM as the acceptor, respectively. The better PCEs were achieved by improving the short-circuit current density without sacrificing the high open-circuit voltage and fill factor through the strategy of incorporating the advantages of both conventional small molecules and polymers for OPVs.

Organic photovoltaics (OPVs) have been considered to be a promising next-generation green technology to address the increasing energy problems worldwide. Currently, OPVs are based on two types of electron donor materials, polymers and small molecules.<sup>1,2</sup> In the past few years, power conversion efficiencies (PCEs) of >9% have been achieved for polymer-based OPVs (P-OPVs) with the most promising bulk-heterojunction (BHJ) architecture.<sup>3</sup> To date, state-of-the-art solution-processed small-molecule-based OPVs (SM-OPVs) have demonstrated PCEs of >7%,<sup>4–6</sup> but their overall performance is still significantly behind that of their polymer counterparts. Obviously, the first issue to close this gap is to design better materials in the active layer.<sup>2,7,8</sup> One issue for SM-OPVs using solution processing used to be the poor film quality, but fortunately, this has been overcome in the last 2–3 years by the rapid development of nonconventional small molecules with appropriate alkyl substituents and relatively long conjugation systems (6–10 units) compared with conventional small molecules. It is important to note that compared with P-OPVs, SM-OPVs enjoy some important advantages, including (1) uniform and defined molecular structures, resulting in less batch-to-batch variation;<sup>9</sup> (2) generally higher open-circuit voltage ( $V_{oc}$ );<sup>8</sup> (3) higher hole mobility than the corresponding polymer materials;<sup>10</sup> and (4) structural versatility with facile control of energy levels via delicate chemical structure designs.<sup>11</sup> Careful analysis of the difference in the best performance of P-OPV and SM-OPV devices indicates that among  $V_{oc}$ , the short-circuit current density ( $J_{sc}$ ), and the fill

factor (FF), the property requiring the most improvement is  $J_{sc}$ . This is based on the following results: (1) the optimized  $V_{oc}$  values for SM-OPVs are generally higher than those of P-OPVs, and their FFs are close to that of the best P-OPV; (2) the  $J_{sc}$  values for SM-OPVs are still far behind those for P-OPVs. Therefore, the question now is how to improve  $J_{sc}$  while retaining the best performance of  $V_{oc}$  and FF for small-molecule donors. These thoughts, combined with the recent and rapid development of both P-OPVs and SM-OPVs,<sup>3,4</sup> prompted us to wonder about the following questions:<sup>12–14</sup> Can we more rationally design small molecules to take maximum advantage of both conventional small molecules and polymers simultaneously and thus achieve better optimized solar cell performance? What building blocks can we borrow from the much richer P-OPV studies to achieve such a goal?

Our recently reported molecule DR3TBDT containing a central alkoxy-substituted benzo[1,2-*b*:4,5-*b'*]dithiophene (BDT) unit (Figure 1a) achieved a PCE of 7.38% with both optimized  $V_{oc}$  (0.93 V) and FF (65%).<sup>5</sup> Thus, is it possible to improve the  $J_{sc}$  while keeping/improving other factors? To this end, we report the design and OPV performance studies of three new small molecules with higher OPV performance: DR3TBDTT, DR3TBDTT-HD, and DR3TBD2T (Figure 1a). First, the BDT unit was chosen as the central building block because of its extended conjugation and planar structure, which make it an efficient unit for high-performance P-OPVs.<sup>15–17</sup> To achieve a higher  $J_{sc}$ , greater conjugation was employed by introducing thiophene or bithiophene units<sup>18</sup> at the 4- and 8-positions of the BDT unit. To enhance the solubility and possibly impact the photovoltaic performance, two different alkyl chains, 2-ethylhexyl and 2-hexyldecyl, were employed on the thiophene units. 3-Ethylrhodanine was again selected as the end unit because our systematic screening of various end units showed it to be the best.<sup>5,14,19,20</sup> The BDT central building block and rhodanine units were then linked by alkyl-substituted terthiophene-based  $\pi$ -conjugated spacers to guarantee good solubility and also to form an effectively long conjugated acceptor–donor–acceptor (A–D–A) backbone structure with strong intramolecular charge transfer and broad absorption, as has been demonstrated recently for SM-OPVs.<sup>5,14,21</sup>

The three new small molecules were synthesized through classical reactions such as Stille coupling, Knoevenagel reaction, and so on, and the synthesis and purification procedures all

Received: April 3, 2013

Published: May 24, 2013

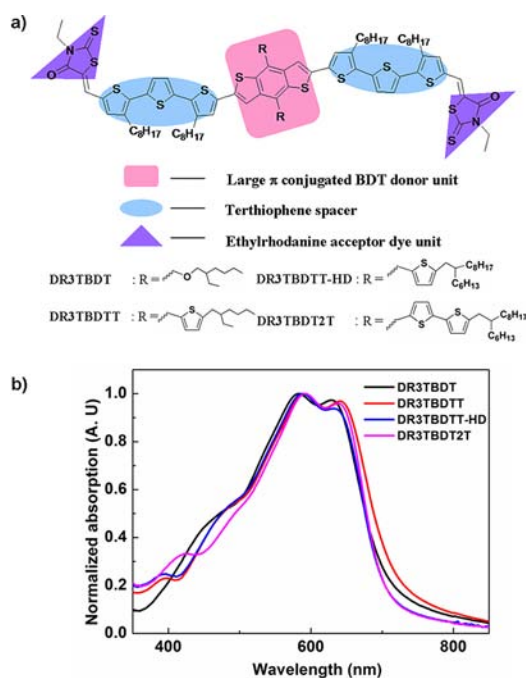


**Figure 1.** (a) Chemical structures of DR3TBDT, DR3TBDTT, DR3TBDTT-HD, and DR3TBD2T. (b) Normalized UV-vis absorption spectra of thin films of these four molecules on quartz.

were well-repeated on the scale of grams in relatively high yields. The purity of the targeted compounds for device fabrication was guaranteed by multiple column purifications and checked by HPLC. The detailed synthetic procedures and characterization data are presented in the Supporting Information (SI). All of them are rather soluble in chloroform, dichlorobenzene, and similar solvents, a prerequisite for solution-processed SM-OPVs. Thermogravimetric analysis (TGA) showed that they exhibit excellent stability, with decomposition temperatures above 400 °C under a N<sub>2</sub> atmosphere (Figure S1 in the SI).

The UV-vis absorption spectra of thin films of DR3TBDT and the three new compounds spin-coated on quartz substrates are presented in Figure 1b. As expected, the larger conjugation resulting from the introduction of the thiophene units on the BDT moiety caused red shifts in the solution UV-vis spectra of the three new compounds compared with DR3TBDT (Figure S2 and Table S1), and similar shifts were observed in the UV-vis spectra of the solid films. For example, the DR3TBDTT film exhibits absorption peaks at 591 and 640 nm, compared with 583 and 630 nm for DR3TBDT. Overall, the film spectra exhibit broad absorption over the range from 300 to 800 nm and have two strong absorption peaks, one of which is a vibronic shoulder, indicating effective  $\pi$ - $\pi$  packing between the molecule backbones. By extrapolation of the absorption onsets in the film state, the optical band gaps were estimated to be 1.74, 1.72, 1.76, and 1.76 eV for DR3TBDT, DR3TBDTT, DR3TBDTT-HD, and DR3TBD2T, respectively, which are consistent with the values of 1.75, 1.75, 1.77, and 1.78 eV, respectively, measured by cyclic voltammetry (CV) (Figure S3). While it is likely that the last digit of the estimated band gap may not be meaningful, compound DR3TBDTT indeed has the lowest band gap. In addition, the three new compounds showed CV-estimated highest occupied molecular orbital (HOMO) and lowest unoccupied MO (LUMO) levels very similar to those of DR3TBDT (Table S1).

Solution-processed BHJ devices were fabricated utilizing [6,6]-phenyl-C<sub>71</sub>-butyric acid methyl ester (PC<sub>71</sub>BM) as the electron acceptor with a conventional BHJ device structure of ITO/PEDOT:PSS/DR3TBDTT:PC<sub>71</sub>BM/LiF/Al. Similar to the case for the earlier compound DR3TBDT, the optimal weight ratio for the three new compounds with PC<sub>71</sub>BM was 1:0.8, and the device performance could be further improved by the addition of a small amount (0.2 mg mL<sup>-1</sup>) of polydimethylsiloxane (PDMS) to the active-material chloroform solution for device fabrication.<sup>22</sup> Other additives such as 1,8-diiodooctane and 1-chloronaphthalene were also tried but did not work well. The optimized device performance parameters for DR3TBDT, DR3TBDTT, DR3TBDTT-HD, and DR3TBD2T devices under AM 1.5G illumination (100 mW cm<sup>-2</sup>) are summarized in Table 1. The average OPV parameters are presented in the Table S2.

**Table 1. Optimized OPV Device Parameters for DR3TBDT, DR3TBDTT, DR3TBDTT-HD, and DR3TBD2T**

donor <sup>a</sup>	V <sub>oc</sub> (V)	J <sub>sc</sub> (mA cm <sup>-2</sup> )	FF (%)	PCE (%)
DR3TBDT <sup>b</sup>	0.93	11.40	65.3	6.92
DR3TBDT <sup>b,c</sup>	0.93	12.21	65.0	7.38
DR3TBDTT	0.91	13.15	62.8	7.51
DR3TBDTT <sup>c</sup>	0.93	13.17	66.3	8.12
DR3TBDTT-HD	0.96	12.36	53.3	6.32
DR3TBDTT-HD <sup>c</sup>	0.96	11.92	59.4	6.79
DR3TBD2T	0.90	11.97	70.4	7.58
DR3TBD2T <sup>c</sup>	0.92	12.09	72.1	8.02

<sup>a</sup>Donor:PC<sub>71</sub>BM weight ratio = 1:0.8. <sup>b</sup>Data from ref 5. <sup>c</sup>PDMS (0.2 mg mL<sup>-1</sup>) was added to the active-material solution.

Before the addition of PDMS, DR3TBDTT and DR3TBD2T with larger conjugation in the orthogonal direction demonstrated high PCEs of 7.51% and 7.58%, respectively (Table 1). However, replacing the 2-ethylhexyl substituents in DR3TBDTT with the bulkier 2-hexyldecyl groups in DR3TBDTT-HD resulted in a lower PCE of 6.32%. This lower PCE for DR3TBDTT-HD corresponds to its lower FF relative to the other three molecules, which is believed to be due to the lower mobility and relatively poor morphology, as discussed below. The OPV devices based on DR3TBDT and the three new molecules all exhibited high V<sub>oc</sub> values of >0.9 V. The especially high V<sub>oc</sub> of 0.96 V for DR3TBDTT-HD with long-alkyl-chain substituents on the thiophene units at the BDT 4- and 8-positions might be caused by the weak intermolecular interactions due to the bulk effect of long alkyl chains.<sup>23</sup> The observed V<sub>oc</sub> values and their trend for these compounds are consistent with modeling results based on the dark current and HOMO/LUMO data (Figure S6 and Table S3). Among these four molecules, DR3TBDTT gave the device with the highest J<sub>sc</sub>, consistent with its most red-shifted absorption and lowest band gap compared with other three molecules. Surprisingly, DR3TBD2T with two thiophene units at both the 4- and 8-positions of the BDT unit gave not only a lower V<sub>oc</sub>, as expected, but also a lower J<sub>sc</sub>; the latter result was unexpected and might be due to the blue shift of DR3TBD2T relative to DR3TBDTT with only one thiophene unit on each side of the BDT unit. Interestingly, however, DR3TBD2T demonstrated the highest FF among the four compounds, which might be attributed to its high and balanced charge mobilities and preferred morphology, as discussed below.

After addition of PDMS, the PCEs of the four molecules all increased (Table 1). Notably, PCEs of 8.12% (Figure 2a) and

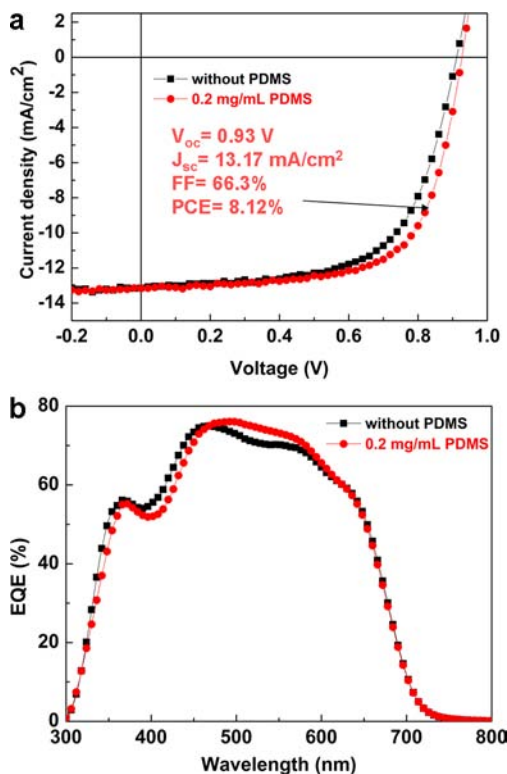


**Figure 2.** (a)  $J$ - $V$  curves and (b) EQE plots for OPV devices based on DR3TBDTT:PC<sub>71</sub>BM (1:0.8 w/w) with (red) and without (black) 0.2 mg mL<sup>-1</sup> PDMS.

8.02% were achieved for DR3TBDTT and DR3TBDT2T, respectively. This was mainly a result of the improved FF, as the FF of DR3TBDT2T reached 72.1%. Indeed, our strategy of replacing the central BDT unit in DR3TBDT with a better unit improved the  $J_{sc}$  without sacrificing the  $V_{oc}$  and FF.<sup>5</sup> The PCEs of >8% are among the highest reported for small-molecule- and polymer-based solar cells.<sup>4,6,24</sup> It is important to note that the device performance of these molecules exhibited good reproducibility (Table S2). For example, the devices made from DR3TBDTT had an average PCE of 7.80% for over 100 devices and a certified PCE of 7.61% after encapsulation with UV epoxy, as determined by the National Center of Supervision and Inspection on Solar Photovoltaic Products Quality (CPVT) of China (Figure S4). The latter value is a downgrade of ~6% due to decreased  $J_{sc}$  and FF compared with that measured in our laboratory, which could be attributed to nonoptimized encapsulation and degradation of the device during the waiting period for certification.

The performance of the above devices was also supported by the results of the external quantum efficiency (EQE) measurements. As shown in Figure 2b and Figure S5, the EQE curves of the three compounds with and without 0.2 mg mL<sup>-1</sup> PDMS exhibited broad and strong responses from 320 to 720 nm. For DR3TBDTT, addition of PDMS obviously improved the EQE values at 470–600 nm, with the remarkable maximum value of 75% at 530 nm (Figure 2b). The calculated  $J_{sc}$  values obtained by integration of the EQE data for DR3TBDTT-, DR3TBDTT-HD-, and DR3TBDT2T-based devices with and without PDMS showed a 2–5% mismatch

compared with the  $J_{sc}$  values from the  $J$ - $V$  measurements (Table S4).

The morphologies of blend films (1:0.8 w/w) of the three molecules with PC<sub>71</sub>BM spin-coated from chloroform solutions with and without PDMS were studied by atomic force microscopy (AFM) (Figure 3 and Figure S7), transmission

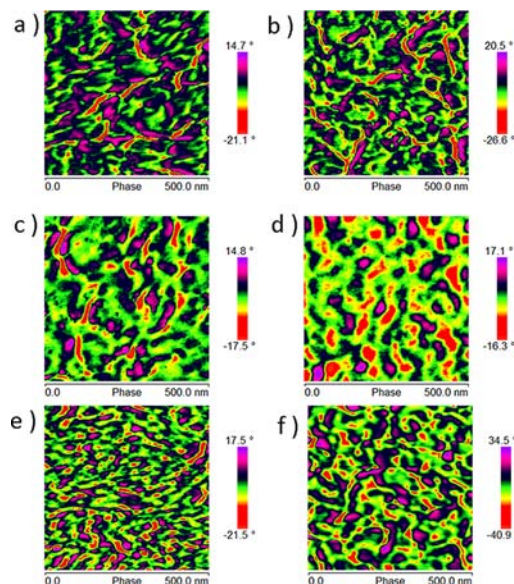


**Figure 3.** Tapping-mode AFM phase images of the active layers of (a, b) DR3TBDTT/PC<sub>71</sub>BM, (c, d) DR3TBDTT-HD/PC<sub>71</sub>BM, and (e, f) DR3TBDT2T (1:0.8 w/w) without (a, c, e) and with (b, d, f) PDMS.

electron microscopy (TEM) (Figure S8), and two-dimensional (2D) grazing-incidence wide-angle X-ray scattering (GIWAXS) (Figure S9). Overall, the blend films for all three compounds with and without PDMS demonstrated rather fine and evenly distributed domains with sizes of tens of nanometers and continuous interpenetrating networks without any observed large aggregates of either the donor or the acceptor. Several notes are worthy of mention. First, AFM showed that the films all had low roughness ( $\lesssim 1$  nm). Second, with addition of PDMS, the domains all slightly increased in size but had smaller roughness, as observed by TEM and AFM [see Table S5 for the domain sizes determined by AFM, TEM, and X-ray diffraction (XRD)]. For example, the domain size measured by AFM for DR3TBDTT increased slightly from 10–30 to 15–40 nm. Also, the interpenetrating D–A networks were improved (AFM, Figure 3; TEM, Figure S8). It has been reported widely that the ideal domain size in the active layer for optimized OPV devices is on the order of tens of nanometers, though more accurate values could be argued and probably depend on the individual case. The optimized domain size should be that which is large enough for an effective continuous interpenetrating D–A charge transport pathway and small enough for efficient exciton separation matching the short effective exciton diffusion length. It could be very likely that the slightly increased domain size with PDMS better matches the above criteria, thus generating an improved FF and PCE, since better interpenetration of the D and A phases is one of the important factors to improve the FF, which is beneficial for exciton separation and charge transport.<sup>2</sup> Third, the DR3TBDTT and DR3TBDT2T films have more even and better morphologies with better interpenetrating networks than DR3TBDTT-HD



(Figure S8), which has the lowest FF. Fourth, in a comparison of the two compounds DR3TBDTT and DR3TBDT2T, the TEM-estimated domain size for DR3TBDTT was 10–15 nm with PDMS, while that for DR3TBDT2T was larger (30–40 nm). The donor domain sizes from 2D XRD for all four compounds were 10–20 nm using the 2D GI-WAXS 100 diffraction peak. Furthermore, the 2D GI-WAXS results also indicated that all of the compounds exhibited a greater preference for edge-on molecular orientation relative to the substrate. It should be noted that the domain size estimation using AFM, TEM, and XRD may have large errors and reflect different film depths. Overall, however, the sizes of tens of nanometers observed using different methods are consistent with the expected ideal domain size of 10–20 nm for OPV devices. These morphology results support the overall high OPV performance of these compounds and are consistent with the observation that DR3TBDTT exhibited the best performance.

On the other hand, the hole and electron mobility measurements on the blends of the three molecules with PC<sub>71</sub>BM with the PMDS additive based on the space-charge limited current (SCLC) model demonstrated balanced hole and electron mobilities (Figures S10–15 and Table S7), especially in the case of DR3TBDT2T, where the most balanced hole and electron mobilities of  $3.29 \times 10^{-4}$  and  $4.19 \times 10^{-4}$  cm<sup>2</sup> V<sup>-1</sup> s<sup>-1</sup>, respectively, were observed. This is also consistent with the higher FF of DR3TBDT2T and the better performance of the devices using this molecule.<sup>25</sup>

In summary, three small molecules incorporating the advantages of both conventional polymers and small molecules synergistically have been designed and synthesized for use in SM-OPVs. For one of them, DR3TBDTT, a high PCE of 8.12% was achieved. This result is among the highest reported for small-molecule- and polymer-based solar cells. This exciting result demonstrates that better solar cell performance for small molecules can indeed be achieved through careful molecule design and device optimization. In view of their versatile structures, we fully believe that there is still great room for designing more favorable small molecules for higher-performance solar cells using our strategy through delicate molecule design and that PCEs of 10% or higher, the landmark value required for possible commercialization of OPVs, can be achieved in a short time.

## ■ ASSOCIATED CONTENT

### 📄 Supporting Information

Detailed synthetic procedures and characterization data for the three new compounds; OPV device fabrication process and data; and additional experimental results. This material is available free of charge via the Internet at <http://pubs.acs.org>.

## ■ AUTHOR INFORMATION

### Corresponding Author

yschen99@nankai.edu.cn

### Author Contributions

†J.Z., Y.Z., and X.W. contributed equally.

### Notes

The authors declare no competing financial interest.

## ■ ACKNOWLEDGMENTS

The authors gratefully acknowledge financial support from the MoST (Grants 2011DFB50300 and 2012CB933401) and the

NSFC (Grants 51273093 and 50933003) and thank beamline BL14B1 (Shanghai Synchrotron Radiation Facility) for providing beam time.

## ■ REFERENCES

- (1) Cheng, Y. J.; Yang, S. H.; Hsu, C. S. *Chem. Rev.* **2009**, *109*, 5868.
- (2) Mishra, A.; Bäuerle, P. *Angew. Chem., Int. Ed.* **2012**, *51*, 2020.
- (3) He, Z.; Zhong, C.; Su, S.; Xu, M.; Wu, H.; Cao, Y. *Nat. Photonics* **2012**, *6*, 593.
- (4) Kyaw, A. K. K.; Wang, D. H.; Gupta, V.; Zhang, J.; Chand, S.; Bazan, G. C.; Heeger, A. J. *Adv. Mater.* **2013**, *25*, 2397.
- (5) Zhou, J.; Wan, X.; Liu, Y.; Zuo, Y.; Li, Z.; He, G.; Long, G.; Ni, W.; Li, C.; Su, X.; Chen, Y. *J. Am. Chem. Soc.* **2012**, *134*, 16345.
- (6) Kyaw, A. K. K.; Wang, D. H.; Gupta, V.; Leong, W. L.; Ke, L.; Bazan, G. C.; Heeger, A. J. *ACS Nano* **2013**, DOI: 10.1021/nm401267s.
- (7) Lin, Y.; Li, Y.; Zhan, X. *Chem. Soc. Rev.* **2012**, *41*, 4245.
- (8) Walker, B.; Kim, C.; Nguyen, T. Q. *Chem. Mater.* **2011**, *23*, 470.
- (9) Sun, Y.; Welch, G. C.; Leong, W. L.; Takacs, C. J.; Bazan, G. C.; Heeger, A. J. *Nat. Mater.* **2012**, *11*, 44.
- (10) Welch, G. C.; Perez, L. A.; Hoven, C. V.; Zhang, Y.; Dang, X. D.; Sharenko, A.; Toney, M. F.; Kramer, E. J.; Thuc-Quyen, N.; Bazan, G. C. *J. Mater. Chem.* **2011**, *21*, 12700.
- (11) Demeter, D.; Rousseau, T.; Leriche, P.; Cauchy, T.; Po, R.; Roncali, J. *Adv. Funct. Mater.* **2011**, *21*, 4379.
- (12) Zhou, J.; Wan, X.; Liu, Y.; Long, G.; Wang, F.; Li, Z.; Zuo, Y.; Li, C.; Chen, Y. *Chem. Mater.* **2011**, *23*, 4666.
- (13) Liu, Y.; Wan, X.; Wang, F.; Zhou, J.; Long, G.; Tian, J.; You, J.; Yang, Y.; Chen, Y. *Adv. Energy Mater.* **2011**, *1*, 771.
- (14) Li, Z.; He, G.; Wan, X.; Liu, Y.; Zhou, J.; Long, G.; Zuo, Y.; Zhang, M.; Chen, Y. *Adv. Energy Mater.* **2012**, *2*, 74.
- (15) Huo, L.; Zhang, S.; Guo, X.; Xu, F.; Li, Y.; Hou, J. *Angew. Chem., Int. Ed.* **2011**, *50*, 9697.
- (16) Dou, L.; You, J.; Yang, J.; Chen, C. C.; He, Y.; Murase, S.; Moriarty, T.; Emery, K.; Li, G.; Yang, Y. *Nat. Photonics* **2012**, *6*, 180.
- (17) Wang, M.; Hu, X.; Liu, P.; Li, W.; Gong, X.; Huang, F.; Cao, Y. *J. Am. Chem. Soc.* **2011**, *133*, 9638.
- (18) Kularatne, R. S.; Sista, P.; Nguyen, H. Q.; Bhatt, M. P.; Biewer, M. C.; Stefan, M. C. *Macromolecules* **2012**, *45*, 7855.
- (19) He, G.; Li, Z.; Wan, X.; Zhou, J.; Long, G.; Zhang, S.; Zhang, M.; Chen, Y. *J. Mater. Chem. A* **2013**, *1*, 1801.
- (20) He, G.; Li, Z.; Wan, X. J.; Liu, Y.; Zhou, J.; Long, G.; Zhang, M.; Chen, Y. *J. Mater. Chem.* **2012**, *22*, 9173.
- (21) Fitzner, R.; Mena-Osteritz, E.; Mishra, A.; Schulz, G.; Reinold, E.; Weil, M.; Körner, C.; Ziehlke, H.; Elschner, C.; Leo, K.; Riede, M.; Pfeiffer, M.; Uhrich, C.; Bäuerle, P. *J. Am. Chem. Soc.* **2012**, *134*, 11064.
- (22) Graham, K. R.; Mei, J.; Stalder, R.; Shim, J. W.; Cheun, H.; Steffy, F.; So, F.; Kippelen, B.; Reynolds, J. R. *ACS Appl. Mater. Interfaces* **2011**, *3*, 1210.
- (23) Yang, L.; Zhou, H.; You, W. *J. Phys. Chem. C* **2010**, *114*, 16793.
- (24) He, Z.; Zhong, C.; Huang, X.; Wong, W. Y.; Wu, H.; Chen, L.; Su, S.; Cao, Y. *Adv. Mater.* **2011**, *23*, 4636.
- (25) Walker, B.; Tomayo, A. B.; Dang, X. D.; Zalar, P.; Seo, J. H.; Garcia, A.; Tantiwivat, M.; Nguyen, T. Q. *Adv. Funct. Mater.* **2009**, *19*, 3063.